Analytical and Bioanalytical Chemistry
https://doi.org/10.1007/s00216-019-01980-2

RESEARCH PAPER

Study of metabolism and identification of productive regions in filamentous fungi via spatially resolved time-of-flight secondary ion mass spectrometry

Lukas Veiter[1,2] · Markus Kubicek[3] · Herbert Hutter[3] · Ernst Pittenauer[3] · Christoph Herwig[1,2] · Christoph Slouka[1,2]

Received: 3 April 2019 / Revised: 20 May 2019 / Accepted: 13 June 2019

Abstract

Filamentous fungi are well-established production hosts that feature a strong interconnection between morphology, physiology, and productivity. For penicillin production in *Penicillium chrysogenum*, industrial processes frequently favor a pellet morphology comprising compact hyphal agglomerates. Inherently these tightly packed entanglements lead to inactive, degrading sections within the pellet's core because of limitations. Optimal process design requires detailed knowledge of the nature of the limitations and localization of productive zones in the biomass, which is generally obtainable through modeling and complex analytical methods such as oxygen microelectrode and histological investigations. Methods that combine physiological and morphological insight are crucial yet scarce for filamentous fungi. In this study, we used time-of-flight secondary ion mass spectrometry in combination with oxygen and glucose tracer substrates, requiring little effort for sample preparation and measurement. Our method is capable of analyzing oxygen and substrate uptake in various morphological structures by the use of ^{18}O as a tracer. In parallel, we can assess productive biomass regions through identification of penicillin mass fragments to simultaneously study oxygen diffusion, substrate incorporation, and productive biomass sections.

Keywords *Penicillium chrysogenum* · Pellet · Oxygen diffusion · Substrate incorporation · Productivity · Time-of-flight secondary ion mass spectrometry

Introduction

Filamentous fungi are important industrial production organisms for a wide range of products ranging from bulk chemicals to therapeutic proteins. Morphology, physiology, and productivity are tightly interlinked [1]. In submerged culture, morphology is generally characterized as either pelleted, consisting of compact hyphal agglomerates, or filamentous, displaying homogeneously dispersed hyphae. In *Penicillium chrysogenum*, hyphal elements undergo agglomeration to form clumps and eventually pellets [2]. These various morphological forms lead to differing biomass characteristics with advantages and disadvantages. Compact pellet morphology facilitates process control regarding rheology, aeration, and agitation. However, limitations in the pellet's core due to diffusion issues with oxygen and the substrate lead to a decline in biomass viability [2–4]. For optimal process design, a compromise between compact and loose morphology is required. To achieve this, comprehensive insight into morphology-dependent incorporation of the substrate and oxygen as well as the identification of productive regions is necessary, and thereby biomass degradation and/or overfeeding can be avoided. There are two ways of gaining insight: modeling approaches and advanced analytical methods.

Published in the topical collection *Advances in Process Analytics and Control Technology* with guest editor Christoph Herwig.

Electronic supplementary material The online version of this article (https://doi.org/10.1007/s00216-019-01980-2) contains supplementary material, which is available to authorized users.

✉ Christoph Slouka
christoph.slouka@tuwien.ac.at

[1] Research Area Biochemical Engineering, Institute of Chemical, Environmental and Bioscience Engineering, Technische Universität Wien, Gumpendorfer Straße 1a, 1060 Vienna, Austria

[2] Christian Doppler Laboratory for Mechanistic and Physiological Methods for Improved Bioprocesses, Technische Universität Wien, Gumpendorfer Straße 1a, 1060 Vienna, Austria

[3] Institute of Chemical Technologies and Analytics, Technische Universität Wien, Getreidemarkt 9/164, 1060 Vienna, Austria

Published online: 22 July 2019

Regarding the link between morphology and productivity, several studies have identified active regions for penicillin production [2]. Growing regions in a long, branching filamentous structure known as hyphae are continuously formed through branching from nongrowing regions. In time, these apical regions become subapical regions with related vacuolization. Penicillin production occurs in the nongrowing cytoplasm, whereas growing regions and degenerated zones are nonproductive [5, 6]. When this hypothesis is expanded to pellets, the outer layer is deemed the productive zone, containing high quantities of cytoplasm [7, 8]. Consequently, productive regions in hyphal agglomerates of *P. chrysogenum* cannot be expected in the outermost, loose entanglements. Analytical methods to verify these hypotheses use oxygen microelectrode measurements. Viable zones within fungal pellets can be characterized by confocal laser scanning microscopy in combination with staining [9, 10].

Secondary ion mass spectrometry (SIMS) is a powerful technique to obtain information on spatially resolved material composition. As a specimen surface is subjected to a primary ion beam, secondary ions reveal elemental and molecular information with high lateral or mass resolution [11, 12]. Application to biological samples is often hindered by limited desorption of ions with $m/z > 500$ and corresponding problems with the measurement of large molecules. Matrix-assisted laser desorption/ionization is regarded as more suitable for large intact biomolecules with very large molecular masses up to 10,000 Da. However, the development of cluster ion sources in the past decade has greatly increased secondary ion yields of high masses [11, 13]. Consequently, applications for biological samples have grown in importance [12]. Of all SIMS methods, nano-SIMS offers the highest lateral resolution (less than 50 nm) but is limited to elemental ions and small fragments [14]. Featuring comparatively good ion detection between 1500 and 2500 Da at a lateral resolution suitable for subcellular structures (approximately 300 nm), time-of-flight SIMS (ToF-SIMS) is a valid alternative [12]. In the field of filamentous fungi, ToF-SIMS has been used to detect and quantify nutrients contained in individual hyphae [15, 16]. An application to study oxygen diffusion and substrate incorporation in specific morphological regions of filamentous biomass is currently unknown to us. For this purpose, the "collimated burst alignment" (CBA) operation mode [17] is highly suitable as it is optimized for oxygen isotope analysis and is capable of sub-100-nm lateral resolution.

In this study, we used ToF-SIMS in CBA operation mode combined with oxygen and glucose tracer substrates to develop a novel analytical method for spatially resolved analysis of substrate and oxygen incorporation into biomass. Additional capabilities include the measurement of spatially resolved precursor incorporation of phenoxyacetic acid for penicillin production in surface biomass regions and identification of productive hyphal areas. To the best of our knowledge, the method presented here is unprecedented in terms of application and broad information gain.

Materials and methods

Strain, medium, and cultivation

Spore suspensions of the P-14 *P. chrysogenum* candidate strain for penicillin production descending from the P-2 *P. chrysogenum* candidate strain (American Type Culture Collection access number ATCC 48271) were provided by Sandoz (Kundl, Austria) and used for all experiments.

All shake-flask cultivations were performed in an Infors HT Multitron shaker (Infors, Bottmingen, Switzerland) at 25 °C and 300 rpm. Fifty milliliters of an autoclaved complex preculture culture medium (sucrose 18 g/l, glucose 3 g/l, corn steep liquor 26 g/l, and $CaCO_3$ 3.8 g/l) in a 500-ml shake flask was inoculated with 1×10^9 spores per milliliter. By convention, after 53.5 h in preculture medium, 10 vol% of preculture broth was transferred to 50 ml of a main-culture medium similarly as described by Posch and Herwig [18].

High-performance liquid chromatography analysis

High-performance liquid chromatography using an UltiMate 3000 system (Thermo Fisher Scientific, MA, USA) with a Zorbax Eclipse AAA C_{18} column (Agilent Technologies, Santa Clara, CA, USA) was used to quantify penicillin V and phenoxyacetic acid concentration with eluents as described elsewhere [19]. A flow rate of 1.0 ml/min was used, and the temperature of the column oven was 30 °C. The wavelength of the UV–vis detector for determining penicillin and phenoxyacetic acid peaks via absorption was set to 210 nm.

Oxygen tracer diffusion experiments

Broth (20–30 ml) from preculture shake-flask cultivations was transferred to a sterile 100-ml vessel equipped with a dissolved oxygen probe (easySense O_2 21, Mettler-Toledo, Switzerland) as well as ports for sterile aeration and sampling. ^{18}O tracer pulses (Campro Scientific, Germany) were applied for 5–10 s until the oxygen partial pressure reached oxygen saturation at a value of more than 99.9%. The isotope enrichment of the oxygen used was 97 atom% ^{18}O, and the O_2 purity was 99.9991%. Over the course of the experiment, the oxygen partial pressure was monitored and additional pulses were applied if the oxygen partial pressure decreased under 10%. Samples were taken after various times up to 24 h, and aliquots for subsequent ToF-SIMS measurement were immediately quenched with liquid nitrogen. As CO_2 is produced in fungal metabolism and our aperture was essentially closed, we checked the pH values of each sample (see Fig. S1). In

general, the pH values of the main-culture medium ranged from 5.8 to 6.5, which would not drastically influence fungal activity as fed-batch bioreactor cultivations of the same strain are performed at similar pH values.

Substrate incorporation experiments

Broth (50 ml) from main-culture shake-flask cultivations was transferred to a custom-made sterile 100-ml vessel equipped with a dissolved oxygen probe (easySense O_2 21, Mettler-Toledo) as well as ports for sterile aeration and sampling. D-[1-^{18}O]glucose (Omicron Biochemicals) was added in an amount to match 10% of the total glucose concentration in the main-culture medium. The dissolved oxygen concentration was maintained at a level higher than 40% by adjustment of the aeration rate. The total cultivation time was 40 h, and samples were taken at 0, 20 and 40 h. Aliquots for subsequent ToF-SIMS measurement were immediately quenched with liquid nitrogen.

Sample preparation and ToF-SIMS measurements

Samples were thawed and 1 ml was centrifuged for 5 min at 50 *g* to generate a loose biomass pellet. Supernatant was removed and the pellet was resuspended in 0.1% w/v saline. This step was repeated; however, 0.01% w/v saline was used for the repeated resuspension. Then 100 μl of resuspended broth was pipetted onto a cut silicone weaver specimen holder. The sample was subsequently subjected to sputtering with a sputter coater (Agar Scientific, UK) at 20 mA and 0.1-mbar oxygen partial pressure, which resulted in 20–50 nm of Au, to inactivate exchange of tracer oxygen with ambient air and to inactivate the biomass metabolism.

Subsequent analysis of the oxygen isotope distribution was performed with a TOF.SIMS 5 instrument (IonTof, Münster, Germany) with 25-kV Bi^+ primary ions (approximately 0.03 pA), 1-kV Cs^+ for sputtering (approximately 75 nA), and a low-energy electron gun (20 V) for charge compensation. Negative secondary ions in the mass range from 1 to 146 u were measured. Areas of 100 μm × 100 μm or smaller were analyzed. For sequential sputtering, a 2-kV Cs^+ sputter gun with a sputter area of 300 μm × 300 μm was used. All measurements were performed in static SIMS conditions. Charge compensation was achieved with 20-eV electrons. The ^{18}O fractions were determined by our operating the instrument in CBA mode. Additional details of the CBA measurement mode used for imaging are given in [17, 20].

Mass spectrometry measurements

Low-resolution mass spectra and low-energy collision-induced dissociation tandem mass spectrometry (MS^2) spectra of penicillin standard and phenoxyacetic acid in solid form were acquired with an Esquire 3000plus 3D-quadrupole ion trap mass spectrometer (Bruker Daltonics, Bremen, Germany) in negative-ion mode by means of electrospray ionization. The mass calibration was done with a commercial mixture of perfluorinated trialkyltriazines (ES tuning mix, Agilent Technologies, Santa Clara, CA, USA). All analytes were dissolved in 1:1 methanol hypergrade LC-MS (Merck, Darmstadt, Germany) and UHQ water to form a concentration of roughly 1 mg/ml. Direct infusion experiments were performed with a model 74900 syringe pump (Cole-Parmer Instrument Company, Vernon Hills, IL, USA) at a flow rate of 5 l/min. Full-scan and low-energy collision-induced dissociation MS^2 scans were measured in the *m*/*z* range from 50 to 500 with the target mass set to the *m*/*z* value of the respective precursor ion. Further experimental conditions included a drying gas temperature of 200 °C, a capillary voltage of 4 kV, a skimmer voltage of 40 V, and octapole and lens voltages according to the target mass set. Mass spectra were averaged during a data acquisition time of 1 min, and one analytical scan consisted of three successive microscans, resulting in 50 and 100 analytical scans, respectively, for final full-scan mass spectra or MS^2 spectra.

Results

We tested two different tracer materials based on oxygen-18, both detectable in high sensitivity by ToF-SIMS within biomass samples. Subsequently we evaluated their applicability for detection of substrate limitations in *P. chrysogenum*.

Oxygen tracer diffusion in *P. chrysogenum* using gaseous $^{18}O_2$

We tested the feasibility of oxygen tracer incorporation in hyphal structures to detect ^{18}O within the fungal biomass to test for oxygen limitation in different fungal regions. We studied different times starting with 15 min to a maximum of 24 h. Only at increased times could ^{18}O be detected in amounts that exceed the natural abundance. The results for 24 h are given in Fig. 1. At ambient temperature of 20 °C, we exposed the cells to 0.103 mol of ^{18}O during the 24 h of the experiment. The $^{18}O/(^{16}O + {}^{18}O)$ fraction in biomass samples is very low, with an average value of 0.0025, as seen in Fig. 1. Oxygen incorporation into biomass can also be estimated in more quantitative terms according to Eq. 1:

$$^{18}\mathrm{O incorporated(mmol)} = \frac{\text{oxygen}}{\text{biomass}} \times \text{totalbiomass(g)} \times \frac{10^3}{18\frac{\text{g}}{\text{mol}}} \times \frac{[^{18}O]}{[^{18}O + {}^{16}O]}, \quad (1)$$

where $\frac{\text{oxygen}}{\text{biomass}}$ is 0.31 for the strain used.

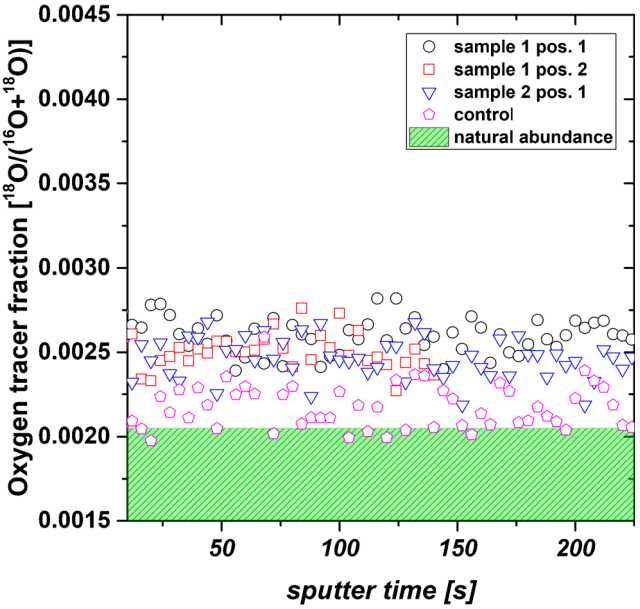

Fig. 1 ^{18}O incorporation normalized to the sum of ^{18}O and ^{16}O after 24 h of incorporation. The values are slightly higher when compared with the control sample and the natural abundance, which indicates almost no incorporation of oxygen through respiration into biomass. Two samples (samples 1 and 2) with ^{18}O incorporation were measured. In sample 1, two distinct positions were analyzed. Furthermore, data from a control sample without ^{18}O as well as natural abundance data are displayed

The previously established average biomass composition of the strain used is 47% C, 7.5% N, 6.5% H, and 31% O. From offline measurements of dry cell weight after 24 h, we can conclude that 0.03 mmol of ^{18}O can be estimated within 1 g of biomass, leaving the vast majority being converted to $C^{18}O_2$. As fixation of the biomass requires evacuation steps, residual $C^{18}O_2$ in the cell is lost as vapor in the preparation and cannot be analyzed subsequently. Hence, the analysis is restricted to oxygen incorporated into biomass. These tracer profiles normalized to the sum of ^{18}O and ^{16}O in the biomass for two samples in three different regions show profiles (see Fig. 1) with only a slight increase of ^{18}O integrated over the entire biomass compared with the natural abundance. The $^{18}O/(^{16}O + {}^{18}O)$ fraction depicted in Fig. 1 increases by $5 \times 10^{-4} \pm 1 \times 10^{-4}$.

As most of the incorporated tracer oxygen is converted to $C^{18}O_2$ gas during the exchange experiment, spatial resolution of viable regions in the fungal structure is not possible with this method. However, it may be used for metabolic flux analysis in combination with mass spectrometry in the gas phase to identify breathing capacity in different process stages during antibiotic production.

Oxygen incorporation into *P. chrysogenum* biomass using ^{18}O-labeled glucose

As incorporation of gaseous tracer oxygen resulted in only very low amounts of incorporation, we used ^{18}O-labeled glucose to test whether changes in the incorporation could be detected on a time-dependent basis and with spatial resolution as displayed in Fig. 2. Samples were taken at three characteristic times: 0, 20 and 40 h. Spatially resolved analysis of the sample after 20 h is presented in Fig. 2. The C_2H_2- signal was used to detect biomass-covered areas on the sample holder (Fig. 2a). Figure 2b shows the total ^{16}O signal in the biomass, and Fig. 2c shows only the incorporated ^{18}O signal originating from the tracer-labeled glucose in the sample.

Despite only 10% of total glucose being tracer-labeled and only one marked oxygen out of six oxygen, a clear spatially resolved image of incorporation could be obtained after 20 h of cultivation (five generation times in nonlimited batch phase). The time dependence of incorporation is given in Fig. 3 for the three different times. The sample at 0 h shows an unexpected increase compared with the natural abundance at first glance. As the medium already contains tracer-labeled glucose, low amounts of medium attached to the surface may cause the deviations in the sample. However, a clear time dependence can be seen from the depth profiles given in Fig. 3, with an increase of about a factor of 1.5 in tracer oxygen content for every 20 h on the basis of Eq. 2:

$$\text{Ratio} = \frac{\left[{}^{18}\text{O}\right]_{t=x} - \text{NA}}{\left[{}^{18}\text{O}\right]_{t=x+20} - \text{NA}}, \tag{2}$$

where NA is the natural abundance.

With a higer number of labeled oxygen atoms in glucose or a higher tracer concentration, a far more sensitive increase could be expected, making exchange times of less than 1 h possible for highly resolved measurements. Expecting a factor 30 when using exclusively tracer oxygen with three labeled oxygen atoms would result in a difference of a factor of 3 within 1 h of exchange. To investigate these results in more quantitative terms, we can use Eq. 1 again and use the average biomass composition of the strain used: 47% C, 7.5% N, 6.5% H, and 31% O. With D-[1-^{18}O]glucose present in the medium, the amount of ^{18}O in 1 g of biomass is 0.01 mmol, and the amount of ^{18}O eventually reaches 0.05 mmol/g after 40 h of cultivation with roughly 2 g of biomass formed. As only 10% of the total glucose used in this experiment was D-[1-^{18}O]glucose and incorporation of oxygen in biomass through respiration is negligible (as shown in the previous section), we can further assume that the $^{18}O/(^{16}O + {}^{18}O)$ fraction would further increase by a factor of 10 if solely D-[1-^{18}O]glucose were used. If we furthermore consider all six oxygen atoms, we can estimate the detection of 3.0 mmol of ^{18}O in 1 g of biomass after 40 h of cultivation. These calculations represent average values across the whole analyzed area from one sample. As our method is capable of measuring much smaller areas in specific morphological regions, these numbers might change. Therefore, comparison between measurement of the total sample area and measurement of a reduced sample area including visualization of morphological regions within the same

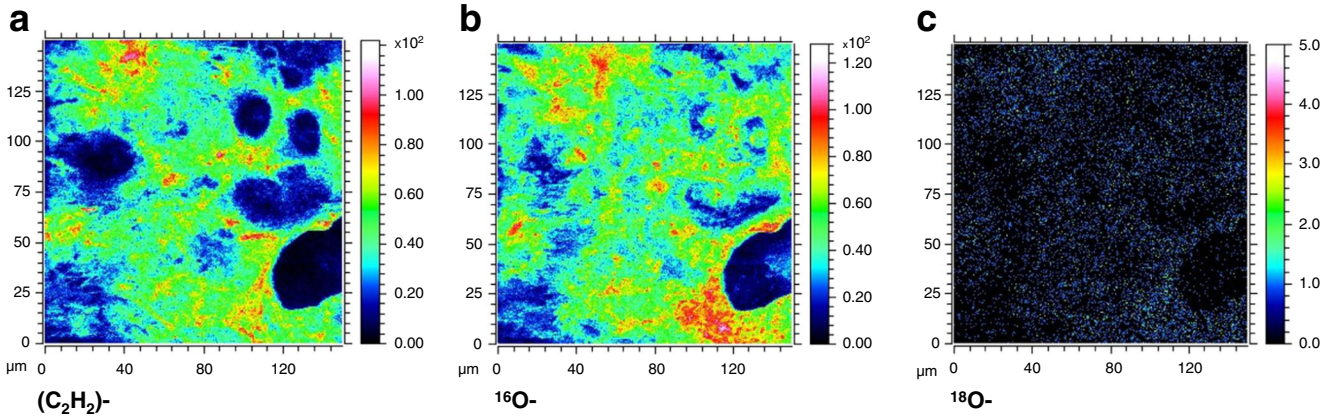

Fig. 2 **a** (C_2H_2)- biomass signal after 20 h of incorporation. **b** (^{16}O)- signal after 20 h of incorporation. **c** (^{18}O)- signal with visible distinct features of the sample. The total ion dose was 8.4×10^{12} cm^{-2}. This measurement as well as the other measurements shown were performed in static secondary ion mass spectrometry conditions

sample or between different samples is possible, as demonstrated in Fig. 4.

This sensitive method of use of tracer-labeled glucose in combination with ToF-SIMS analysis is capable of visualizing metabolically active biomass regions in filamentous biomass. Such information can be used to generate flux-based models for C-source incorporation in biomass and in secondary metabolites (antibiotics) in the different growth phases of fungal cultivation. As of now, industrial processes tend to favor a pellet morphology for reasons of facilitated process control. Therefore, detailed information on limitations within the pellet's core may be accessible with this method. For this purpose, the workflow for sample preparation must include fixation with resin and cutting by ultramicrotomy and subsequent tracer analysis of the corresponding core sections.

Localization of productive regions in *P. chrysogenum* biomass

In addition to oxygen diffusion and incorporation, we studied additional fragment masses obtained in measurement. We observed several prominent fragment masses apart from oxygen, including the carbon backbone in various forms (11 C-, 25 C_2H_2-, 14 CH_2-), as well as a distinct *m/z* 93 fragment consistently localized in the inner sections of the hyphal carbon backbone. This fragment mass varied in intensity according to the sampling time, as well as the penicillin and phenoxyacetic acid concentrations. On the basis of this observation and in accordance with the literature [5–7], we hypothesized that the observed *m/z* 93 fragment must be related to penicillin production. To further verify this hypothesis, we acquired low-

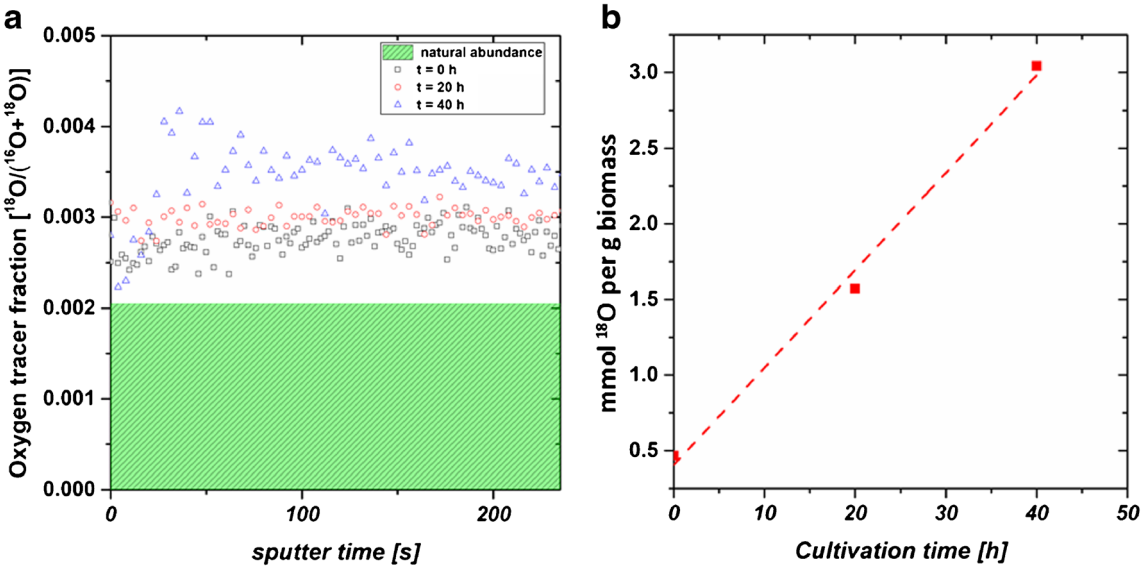

Fig. 3 **a** Time-dependence of ^{18}O tracer incorporation by tracer-labeled glucose. No depth profile can be seen from the measurement, but rather the overall tracer incorporation can be seen. The offset at 0 h compared with the natural abundance is caused by the medium, already containing tracer-labeled glucose. **b** Amount of ^{18}O detected in 1 g of biomass over the cultivation time and the corresponding linear fit

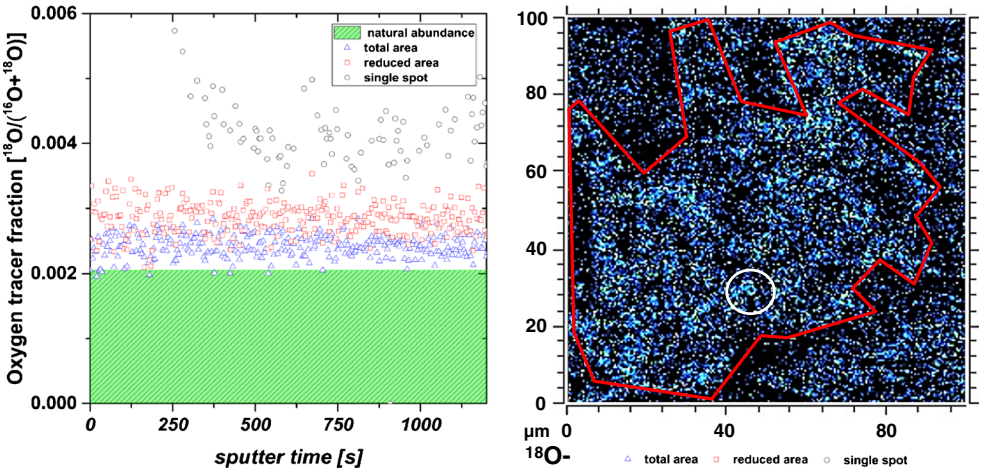

Fig. 4 Measurement of oxygen tracer fraction $^{18}O/(^{18}O + ^{16}O)$ in a reduced sample area, and a single spot, and visualization of the measurement areas within the same sample

resolution mass spectra in negative-ion mode by means of electrospray ionization of penicillin standard and phenoxyacetic acid in solid form and identified the *m/z* 93 fragment in both compounds. In addition, we performed ToF-SIMS measurements of both compounds and also detected the *m/z* 93 fragment. Mass spectra of phenoxyacetic acid and penicillin V are shown in Fig. S2. In Fig. 5a the ratio of the aforementioned *m/z* 93 fragment signal to the $[(C_2H_2)\text{-}]$ (*m/z* 26) signal is displayed for different sampling times integrated over the entire region of interest. High-performance liquid chromatography measurements of the supernatant display increasing penicillin concentration with cultivation time, and the ratio of *m/z* 93 and *m/z* 26 signals obtained from the biomass samples follows the same trend as seen in Fig. 5b, as phenoxyacetic acid is incorporated by the biomass and penicillin is produced accordingly. Obviously, an increased amount of both species is present in the fungal biomass at longer cultivation times. The results from ToF-SIMS measurements are shown in Fig. 6. At long cultivation times, productive zones are clearly indicated by *m/z* 93 fragment signals, mainly in dense hyphal entanglements, and can be furthermore spatially resolved.

The *m/z* 93 fragment in both cases most likely is phenol (C_6H_5O)- present in phenoxyacetic acid and penicillin. With this method is it possible to detect penicillin-producing regions within the hyphal and pellet structure of *P. chrysogenum*. This is in accordance with the literature, as these productive regions are not located in the hyphal tips, but rather occur in nongrowing (subapical) regions [5, 6].

Discussion

We implemented a novel method for spatially resolved analysis of substrate and oxygen incorporation into biomass. The novelty of this approach lies in the application of ToF-SIMS in combination with oxygen and glucose tracer substrates in a new context. In general, such techniques are used in surface science. In this contribution, we demonstrated the feasibility for detailed analysis of substrate uptake in filamentous *P. chrysogenum* biomass with complex morphology. Moreover, our results also suggest that biomass regions involved in penicillin production can be identified.

Advantages, disadvantages, and comparability of the method

The method described here has been used in a novel context to study respiration and substrate incorporation in complex filamentous biomass. It uses ToF-SIMS in CBA operation mode [17], an imaging mode optimized for $^{18}O/^{16}O$ isotope analysis. The approximately 100-nm lateral resolution allows detailed analysis of morphological substructures such as hyphae. This method can clearly distinguish between metabolically active and metabolically nonactive biomass zones, which is especially important for processes in filamentous fungi featuring hyphal agglomerates or pellet structures. Incorporation of oxygen into hyphal structures can be detected when the sample is subjected to ^{18}O for sufficiently long times (more than 12 h). With the use of D-[1-^{18}O]glucose, we can visualize substrate uptake in different biomass regions. Furthermore, we can identify productive zones in detail as demonstrated in Fig. 6 by zooming into productive and nonproductive hyphae.

In this particular method, ToF-SIMS analysis is done with Bi^+ ions. This mode of measurement was specifically chosen for $^{18}O/^{16}O$ isotope analysis, where high fragmentation is helpful. We also found that we can obtain valuable information from higher-mass fragments. For sole analysis of organic mass fragments, higher Bi clusters (e.g., Bi_3^+ or Bi_5^+) or gas cluster guns would be superior to ensure less fragmentation and a higher secondary ion count [13].

Nano-SIMS has higher lateral resolution than ToF-SIMS but ToF-SIMS is still a valid compromise for our method

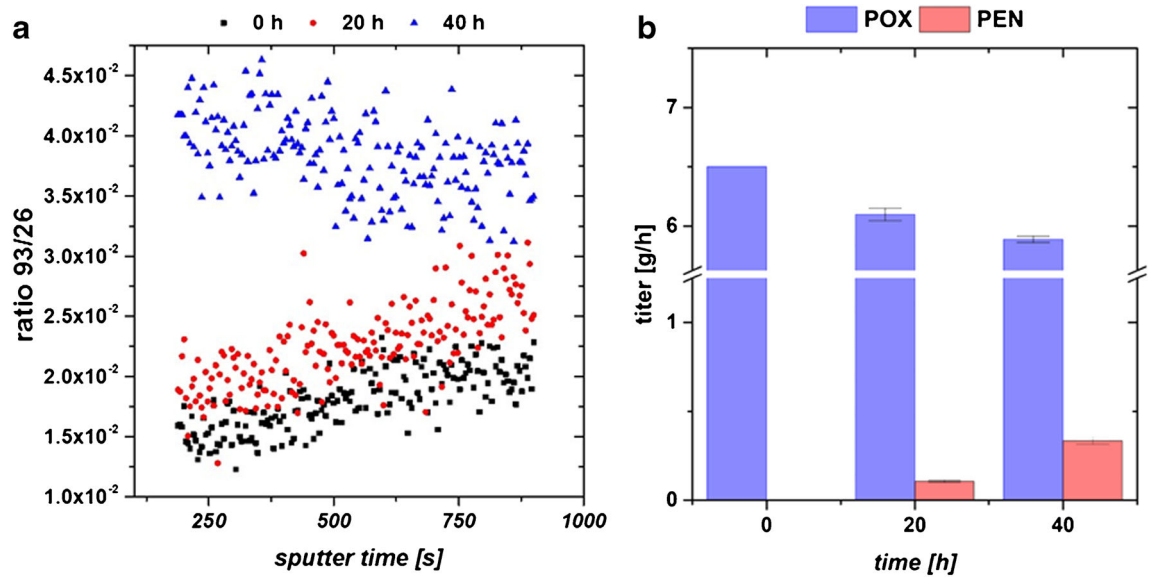

Fig. 5 **a** Time-of-flight secondary ion mass spectrometry measurements: secondary ion ratio of *m*/*z* 93 signal to *m*/*z* 26 signal [C_2-] versus sputter time for three different cultivation times (0, 20 and 40 h). The ratio of the intensity of the *m*/*z* 93 signal (phenol) and the *m*/*z* 26 signal [(C_2H_2-)] demonstrates that the *m*/*z* 93 signal increases in relation to the signal corresponding to the C_2H_2 backbone with cultivation time and penicillin production. **b** High-performance liquid chromatography measurements: concentration of penicillin (PEN) and phenoxyacetate (POX) in the supernatant for three different cultivation times (0, 20 and 40 h)

because of the possibility to study large areas of several hundred micrometers across to study different hyphae simultaneously and because it offers the possibility to measure with low ion doses of less than 10^{13} cm^{-2} to retain static measurement conditions as done for the measurements presented here.

Applicability of the method

Filamentous fungi comprise several morphological forms, affecting biomass viability and productivity in different ways. Whenever the pellet form is favored, detailed knowledge of the pellet's inherent viable, nonviable, and productive zones is essential for process optimization. We envision our method as a tool to facilitate industrial process design and strain characterization by shedding light on C-source incorporation and respiratory limitations within complex fungal biomass agglomerates. This information could also be used in the generation of flux-based models. An additional benefit is the simultaneous localization of productive biomass regions, which does not require further effort in sample preparation or measurement.

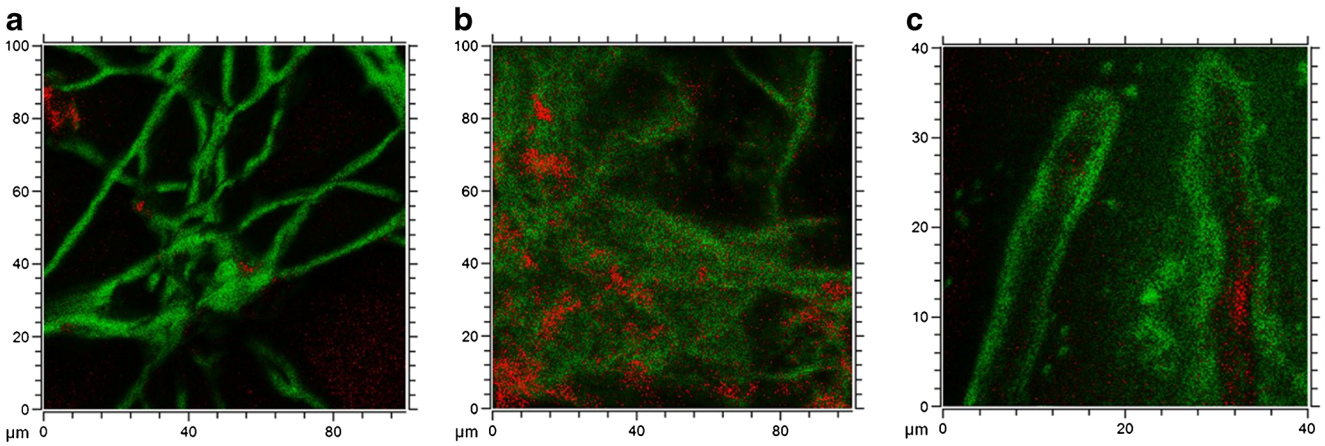

Fig. 6 Time-of-flight secondary ion mass spectrometry measurements with spatial resolution. **a** Hyphal entanglement at a cultivation time of 20 h; overlay of *m*/*z* 26 [(C_2H_2)-] (green) and *m*/*z* 93 [(C_6H_5O)-] (red) signals. **b** Dense hyphal entanglement; overlay of *m*/*z* 26 [C_2H_2-] and *m*/*z* 93 [(C_6H_5O)-] signals at a cultivation time of 40 h. **c** Zoom into productive and nonproductive hyphae at a cultivation time of 20 h; overlay of *m*/*z* 26 [(C_2H_2)-] and *m*/*z* 93 [(C_6H_5O)-] signals

Acknowledgements We thank the Austrian Federal Ministry of Science, Research and Economy through the Christian Doppler Laboratory for financial support. Strains for the experiments were gratefully provided by Sandoz (Kundl, Austria).

Author contributions LV and CS designed the study, performed the experiments, analyzed the data, and wrote the article. MK performed and analyzed the ToF-SIMS measurements. EP performed mass spectrometry measurements. HH provided valuable scientific input. CH supervised the work.

Funding This study was funded by Austrian Federal Ministry of Science, Research and Economy through the Christian Doppler Laboratory for Mechanistic and Physiological Methods for Improved Bioprocesses (grant number 171).

Compliance with ethical standards

Conflict of interest The authors declare that they have no competing interests.

Ethics approval This article does not contain any studies with human participants or animals performed by any of the authors.

References

1. Veiter L, Rajamanickam V, Herwig C. The filamentous fungal pellet-relationship between morphology and productivity. Appl Microbiol Biotechnol. 2018;102(7):2997–3006.
2. Nielsen J, Krabben P. Hyphal growth and fragmentation of *Penicillium chrysogenum* in submerged cultures. Biotechnol Bioeng. 1995;46(6):588–98.
3. Walisko R, Moench-Tegeder J, Blotenberg J, Wucherpfennig T, Krull R. The taming of the shrew - controlling the morphology of filamentous eukaryotic and prokaryotic microorganisms. Adv Biochem Eng Biotechnol. 2015;149:1–27.
4. Zhang J, Zhang J. The filamentous fungal pellet and forces driving its formation. Crit Rev Biotechnol. 2016;36(6):1066–77.
5. Paul GC, Thomas CR. Characterisation of mycelial morphology using image analysis. Adv Biochem Eng Biotechnol. 1998;60:1–59.
6. Zangirolami TC, Johansen CL, Nielsen J, Jorgensen SB. Simulation of penicillin production in fed-batch cultivations using a morphologically structured model. Biotechnol Bioeng. 1997;56(6):593–604.
7. Wittler R, Baumgartl H, Lubbers DW, Schugerl K. Investigations of oxygen-transfer into *Penicillium chrysogenum* pellets by microprobe measurements. Biotechnol Bioeng. 1986;28(7):1024–36.
8. Baumgartl H, Wittler R, Lubbers DW, Schugerl K. Oxygen profiles and structure of *Penicillium chrysogenum* pellets. Adv Exp Med Biol. 1984;169:793–9.
9. Hille A, Neu TR, Hempel DC, Horn H. Effective diffusivities and mass fluxes in fungal biopellets. Biotechnol Bioeng. 2009;103(6):1202–13.
10. Hille A, Neu TR, Hempel DC, Horn H. Oxygen profiles and biomass distribution in biopellets of *Aspergillus niger*. Biotechnol Bioeng. 2005;92(5):614–23.
11. Walker AV. Why is SIMS underused in chemical and biological analysis? Challenges and opportunities. Anal Chem. 2008;80(23):8865–70.
12. Fearn S. Characterisation of biological material with ToF-SIMS: a review. Mater Sci Technol. 2015;31(2):148–61.
13. Kayser S, Rading D, Moellers R, Kollmer F, Niehuis E. Surface spectrometry using large argon clusters. Surf Interface Anal. 2013;45(1):131–3.
14. Nunez J, Renslow R, Cliff JB 3rd, Anderton CR. NanoSIMS for biological applications: current practices and analyses. Biointerphases. 2017;13(3):03B301.
15. Cliff JB, Gaspar DJ, Bottomley PJ, Myrold DD. Exploration of inorganic C and N assimilation by soil microbes with time-of-flight secondary ion mass spectrometry. Appl Environ Microbiol. 2002;68(8):4067–73.
16. Couturier M, Navarro D, Chevret D, Henrissat B, Piumi F, Ruiz-Duenas FJ, et al. Enhanced degradation of softwood versus hardwood by the white-rot fungus Pycnoporus coccineus. Biotechnol Biofuels. 2015;8:216.
17. Kubicek M, Holzlechner G, Opitz AK, Larisegger S, Hutter H, Fleig J. A novel ToF-SIMS operation mode for sub 100 nm lateral resolution: application and performance. Appl Surf Sci. 2014;289:407–16.
18. Posch AE, Herwig C. Physiological description of multivariate interdependencies between process parameters, morphology and physiology during fed-batch penicillin production. Biotechnol Prog. 2014;30(3):689–99.
19. Ehgartner D, Fricke J, Schroder A, Herwig C. At-line determining spore germination of Penicillium chrysogenum bioprocesses in complex media. Appl Microbiol Biotechnol. 2016;100(20):8923–30.
20. Holzlechner G, Kubicek M, Hutter H, Fleig J. A novel ToF-SIMS operation mode for improved accuracy and lateral resolution of oxygen isotope measurements on oxides. J Anal Atom Spectrom. 2013;28(7):1080–9.